eLIFE elifesciences.org

RESEARCH ARTICLE

Figures and figure supplements

Wnt11 directs nephron progenitor polarity and motile behavior ultimately determining nephron endowment

Lori L O'Brien *et al*

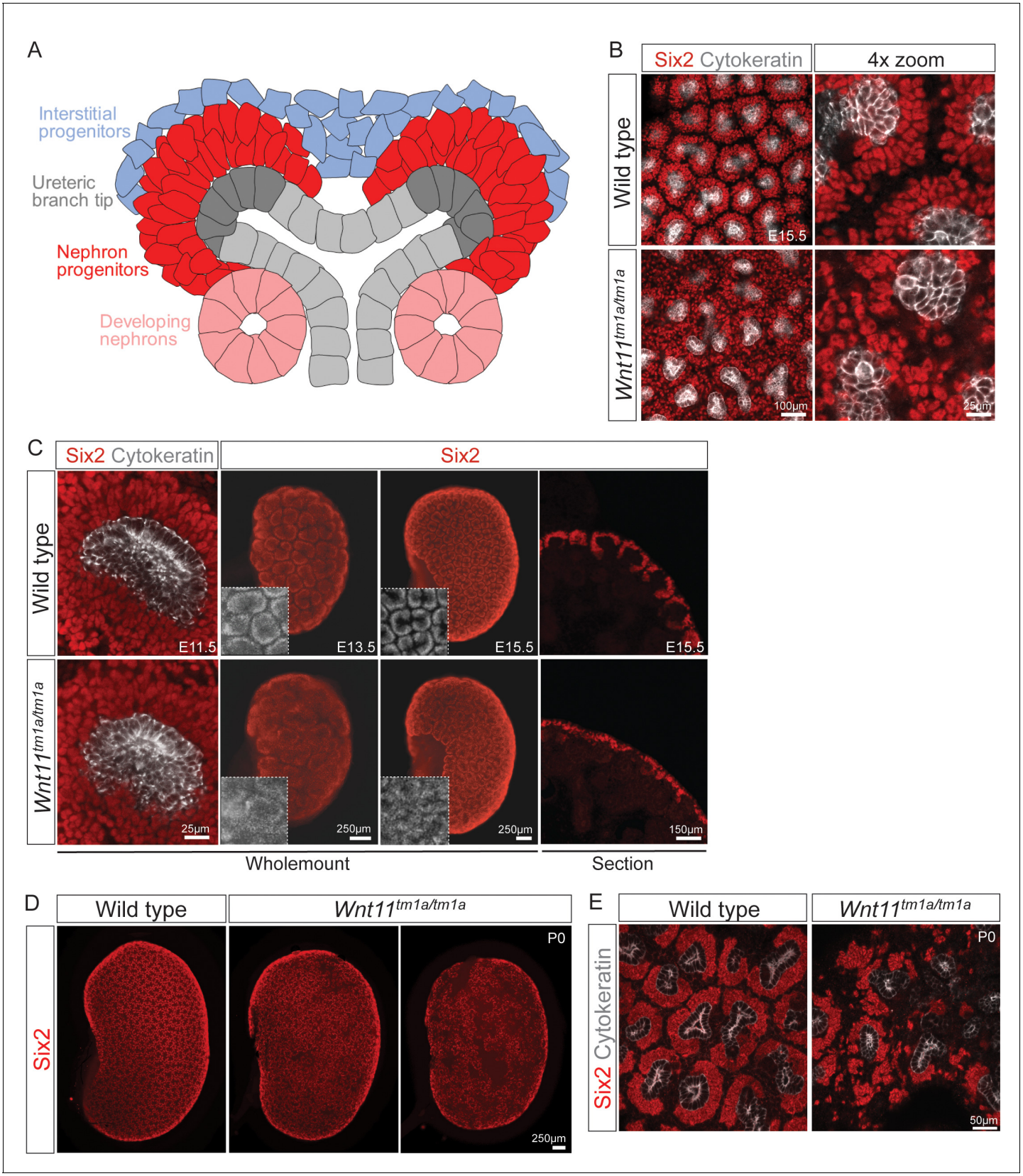

Figure 1. *Wnt11* mutants have persistent loose, disorganized nephron progenitor niches that prematurely dropout. (**A**) Schematic of the nephrogenic niche. Wnt11 is secreted by the ureteric branch tip cells. (**B**) Wholemount immunostained kidneys were analyzed at E15.5. Confocal images show that

Figure 1 continued on next page

Figure 1 continued

Wnt11$^{tm1a/tm1a}$ Six2 +nephron progenitors (red) are dispersed from the ureteric branch tips (grey) and rounded in appearance compared to wild type cells. A 4x zoom in the far-right panel highlights the differences in cellular distribution and morphology. (**C**) Wholemount immunostained wild type and *Wnt11* mutant kidneys were analyzed at E11.5, E13.5, and E15.5. *Wnt11*$^{tm1a/tm1a}$ Six2 +nephron progenitors are more rounded and less organized than wild type counterparts beginning at E11.5 (view shows slice from a z-stack). The disorganized phenotype is clear in whole kidney views (maximum intensity projection) at E13.5 and E15.5. Insets highlight the disorganization in whole kidney views. The far-right panel shows a cryosection of E15.5 wild type and *Wnt11* mutant kidneys immunostained for Six2, highlighting the dispersed phenotype is also evident in section. (**D**) Wholemount immunostains of P0 kidneys show the persistent disorganized phenotype and associated premature dropout of Six2 +nephron progenitor niches (red). (**E**) High resolution confocal views highlight the premature dropout of Six2 +nephron progenitor niches (red) around cytokeratin +ureteric epithelium (grey) in *Wnt11*$^{tm1a/tm1a}$ kidneys.

DOI: https://doi.org/10.7554/eLife.40392.002

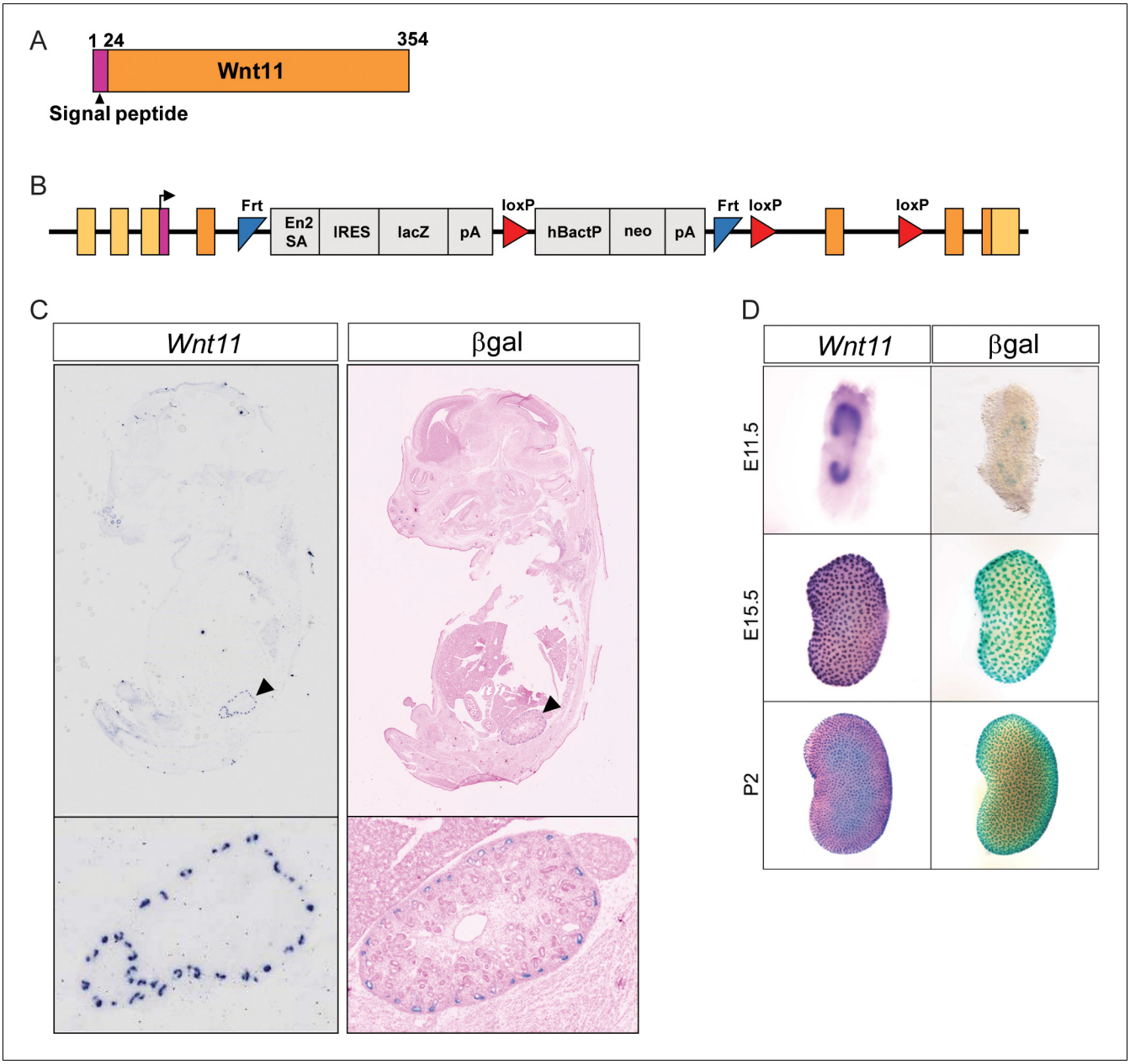

Figure 1—figure supplement 1. The *Wnt11*^{tm1a} allele recapitulates expression of *Wnt11*. (**A**) Schematic of Wnt11 protein. (**B**) Schematic of the *Wnt11*^{tm1a} allele. The coding region is reflected by the colors which correlate with the protein structure depicted in A). (**C**) *Wnt11*$^{tm1a/+}$ tissue sections through a whole E15.5 embryo were subjected to in situ hybridization for *Wnt11* or β-galactosidase staining. The lacZ reporter in the *Wnt11*^{tm1a} allele recapitulates expression of *Wnt11*. (**D**) Kidneys from E11.5, E15.5, and P2 animals were processed for in situ hybridization for *Wnt11* or β-galactosidase staining. The *Wnt11*^{tm1a} allele recapitulates expression of *Wnt11* in the ureteric branch tips throughout development.

DOI: https://doi.org/10.7554/eLife.40392.003

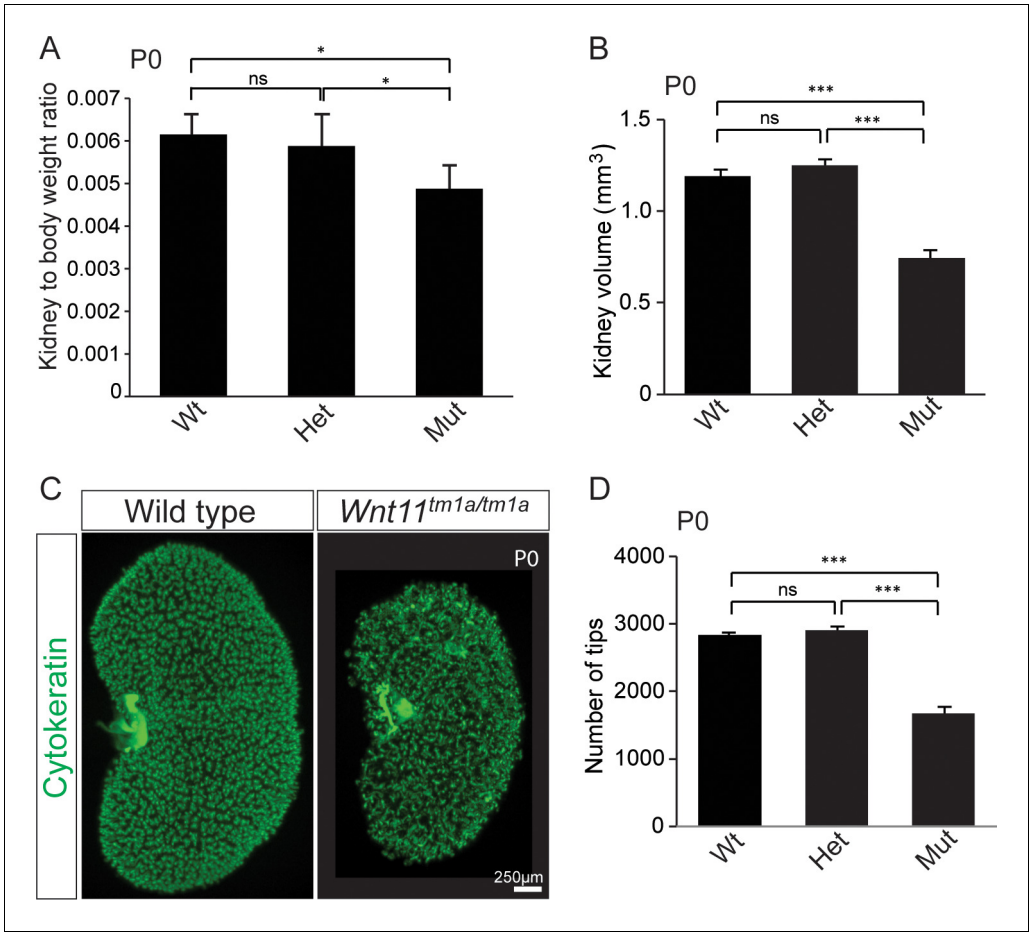

Figure 1—figure supplement 2. Kidney metrics at P0 reveal deficits in *Wnt11* mutants. (**A**) Quantitation of kidney to body weight ratio at P0 shows a significant reduction in *Wnt11* mutants compared to either wild type or heterozygous animals. Error bars show standard deviation (SD) from 6 samples of each genotype. (**B**) Quantitation of kidney volume at P0 by three dimensional analyses show that *Wnt11* mutant kidneys are smaller, error bars represent standard error mean (SEM) from 8 kidneys of each genotype. (**C**) Staining of the P0 ureteric tree with cytokeratin (green) reveals the small kidney structure and reduced branching present in *Wnt11* mutants. (**D**) Quantitation of cytokeratin +ureteric branch tips at P0 by confocal analyses reveals a deficit in *Wnt11* mutants, error bars are SEM from 8 kidneys of each genotype. All significance values were determined by t-test. ns = $p > 0.05$, * = $p < 0.05$, ** = $p < 0.01$, *** = $p < 0.001$.

DOI: https://doi.org/10.7554/eLife.40392.004

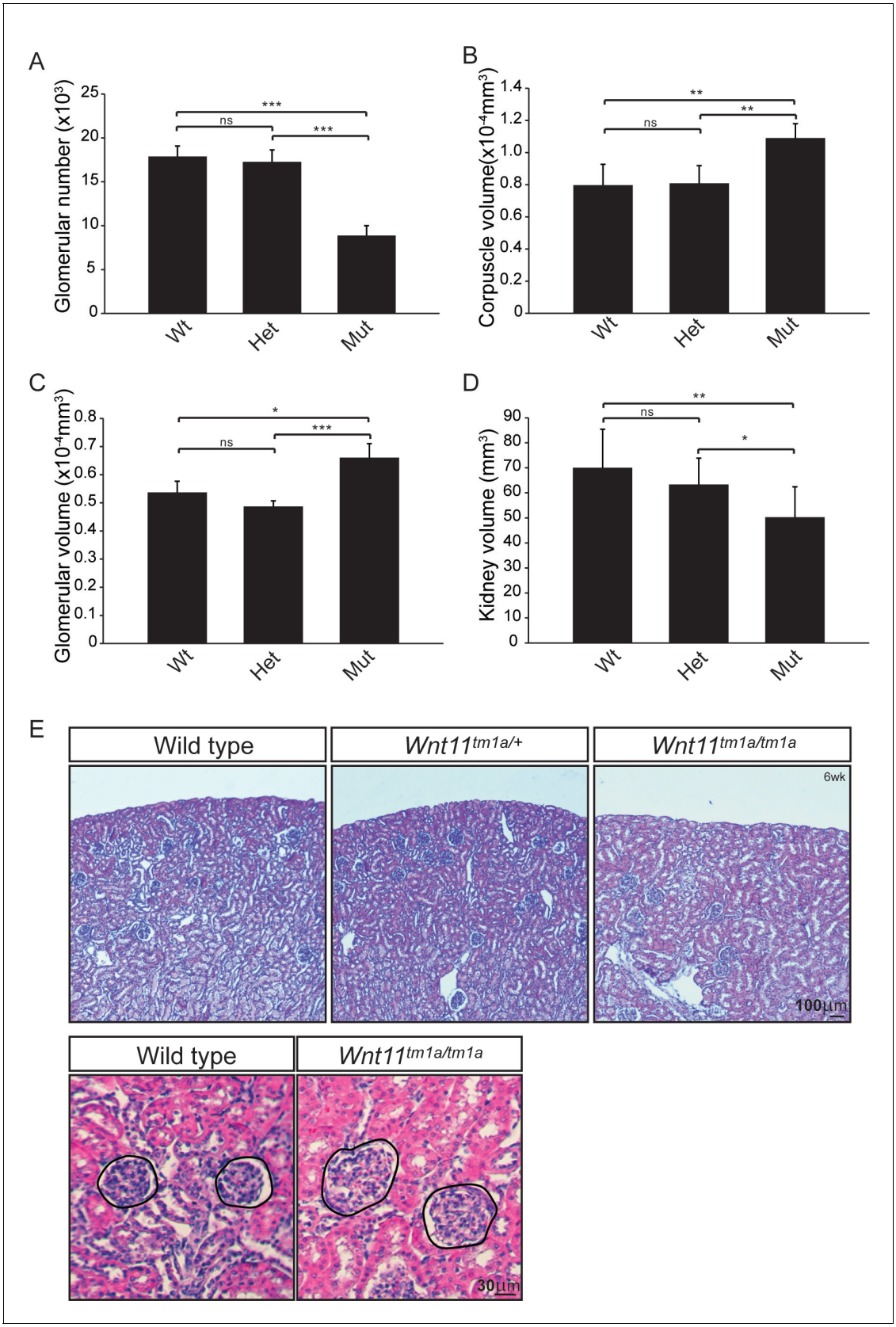

Figure 2. Nephron numbers are reduced in *Wnt11*$^{tm1a/tm1a}$ adults leading to compensatory hypertrophy. (**A**) The physical disector/fractionator method was used to estimate glomerular number in 6 week old animals. A significant reduction is found in *Wnt11* mutants. (**B**) Renal corpuscle volume is

Figure 2 continued on next page

Figure 2 continued

increased in *Wnt11* mutant kidneys. (**C**) Glomerular volume is larger in *Wnt11*$^{tm1a/tm1a}$ kidneys. (**D**) Estimated kidney volume is reduced in *Wnt11* mutants. (**E**) Histological sections stained with hematoxylin and eosin highlight that overall morphology is preserved, although glomerular/corpuscle volume is increased in the *Wnt11* mutants. All error bars represent SEM. All significance values were determined by t-test. ns = $p > 0.05$, * = $p < 0.05$, ** = $p < 0.01$, *** = $p < 0.001$. n = 6 for each genotype.

DOI: https://doi.org/10.7554/eLife.40392.006

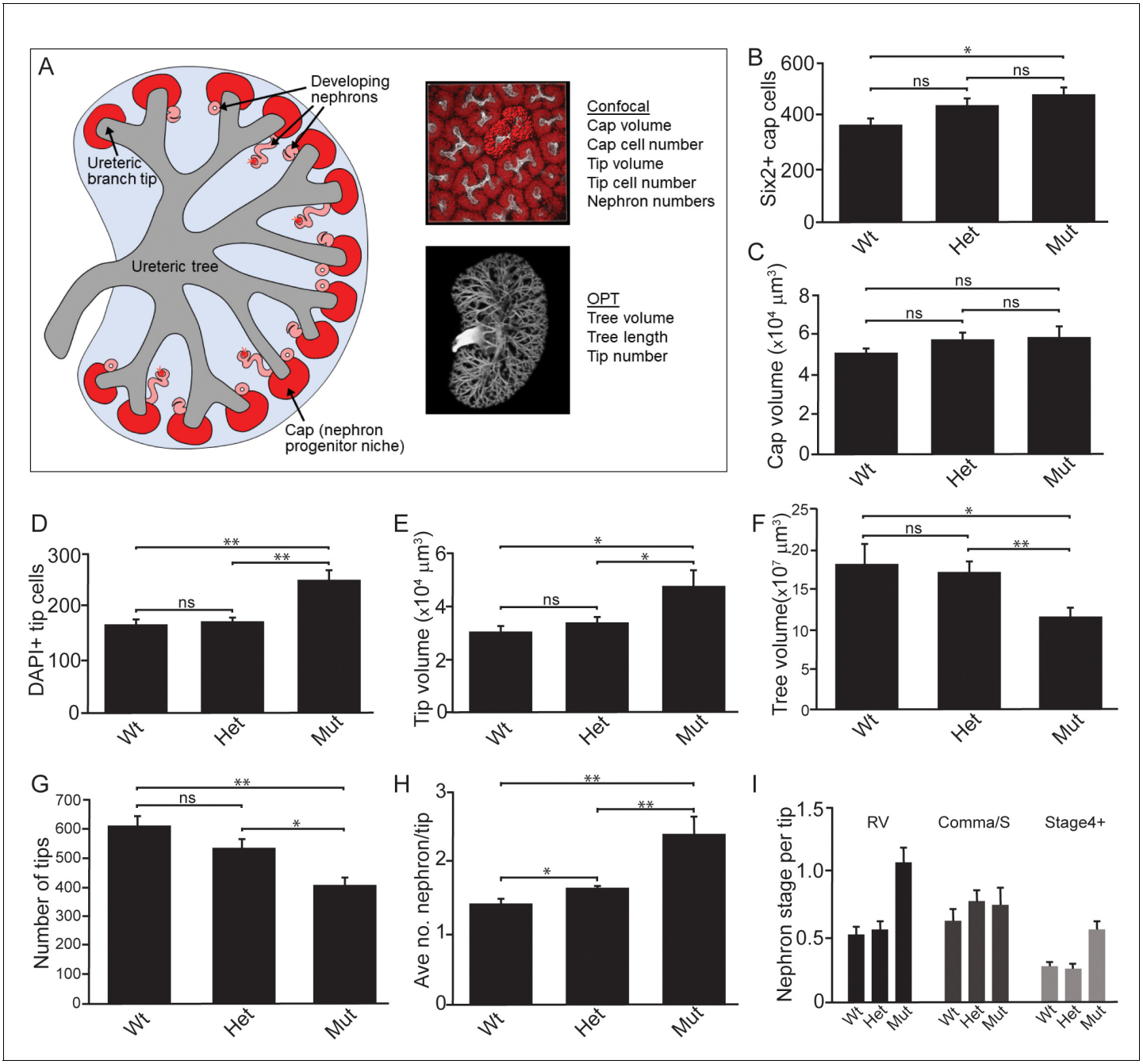

Figure 3. Quantitative analyses reveal significant alterations to niche metrics and accelerated nephrogenesis in *Wnt11*$^{tm1a/tm1a}$ kidneys. (**A**) Schematic of the developing kidney highlighting the niche and structure metrics quantified after imaging by either confocal or optical projection tomography (OPT). E15.5 wholemount immunostains were performed with α-Six2 and α-pan cytokeratin antibodies and kidneys subsequently imaged by confocal microscopy for analyses in B-E, H, and I or OPT for analyses in F-G. (**B**) The number of Six2 +nephron progenitors per niche were quantified and reveal an increase in *Wnt11* mutants. (**C**) The overall volume of each nephron progenitor niche (cap) is not significantly different between wild type and *Wnt11* mutants. (**D**) The number of DAPI +cells were quantified in each cytokeratin +ureteric branch tip niche and were increased in *Wnt11* mutants. (**E**) Ureteric branch tip volumes were measured and are larger in *Wnt11* mutants, correlating with the increase in tip number. (**F**) Ureteric tree volume was quantified and is reduced in *Wnt11*$^{tm1a/tm1a}$ kidneys. (**G**) Quantitation of ureteric branch tip number reveals a significant decrease in *Wnt11*$^{tm1a/tm1a}$ kidneys. (**H**) The average number of nephrons per ureteric branch tip are increased in *Wnt11* mutant kidneys. (**J**) Classification of the developing nephron structures associated with each tip highlight a bias in *Wnt11* mutants towards renal vesicles (RV) and stage 4 + nephrons versus comma/s-shaped bodies. All error bars represent SEM. All significance values were determined by t-test. ns = $p > 0.05$, * = $p < 0.05$, ** = $p < 0.01$, *** = $p < 0.001$. n = 6 kidneys of each genotype for confocal analyses. N = 8 of each genotype for OPT analyses.

DOI: https://doi.org/10.7554/eLife.40392.008

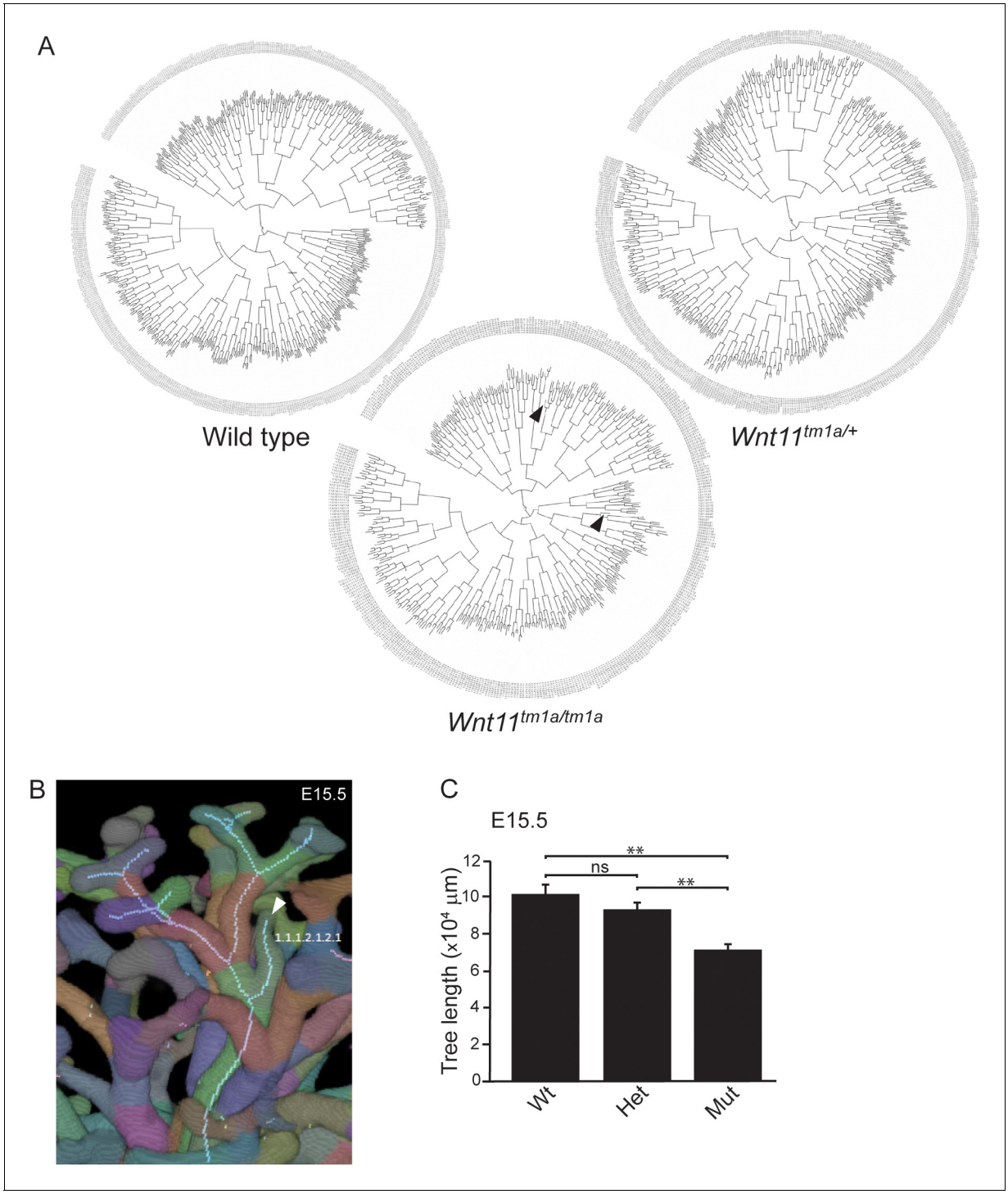

Figure 3—figure supplement 1. Branching patterns are similar among genotypes despite smaller ureteric trees and premature branch truncations in *Wnt11* mutants. (**A**) Clade diagrams of the branching patterns of a representative E15.5 kidney from wild type, *Wnt11*$^{tm1a/+}$, and *Wnt11*$^{tm1a/tm1a}$ animals. Arrowheads point to tips that stopped branching prematurely. (**B**) Optical projection tomography (OPT) image rendered Tree Surveyor highlighting a prematurely truncated branch tip (arrowhead) in a *Wnt11* mutant. (**C**) Ureteric tree length was measured with Tree Surveyor software and is decreased in mutant kidneys. All significance values were determined by t-test. ns = $p > 0.05$, * = $p < 0.05$, ** = $p < 0.01$, *** = $p < 0.001$.
DOI: https://doi.org/10.7554/eLife.40392.009

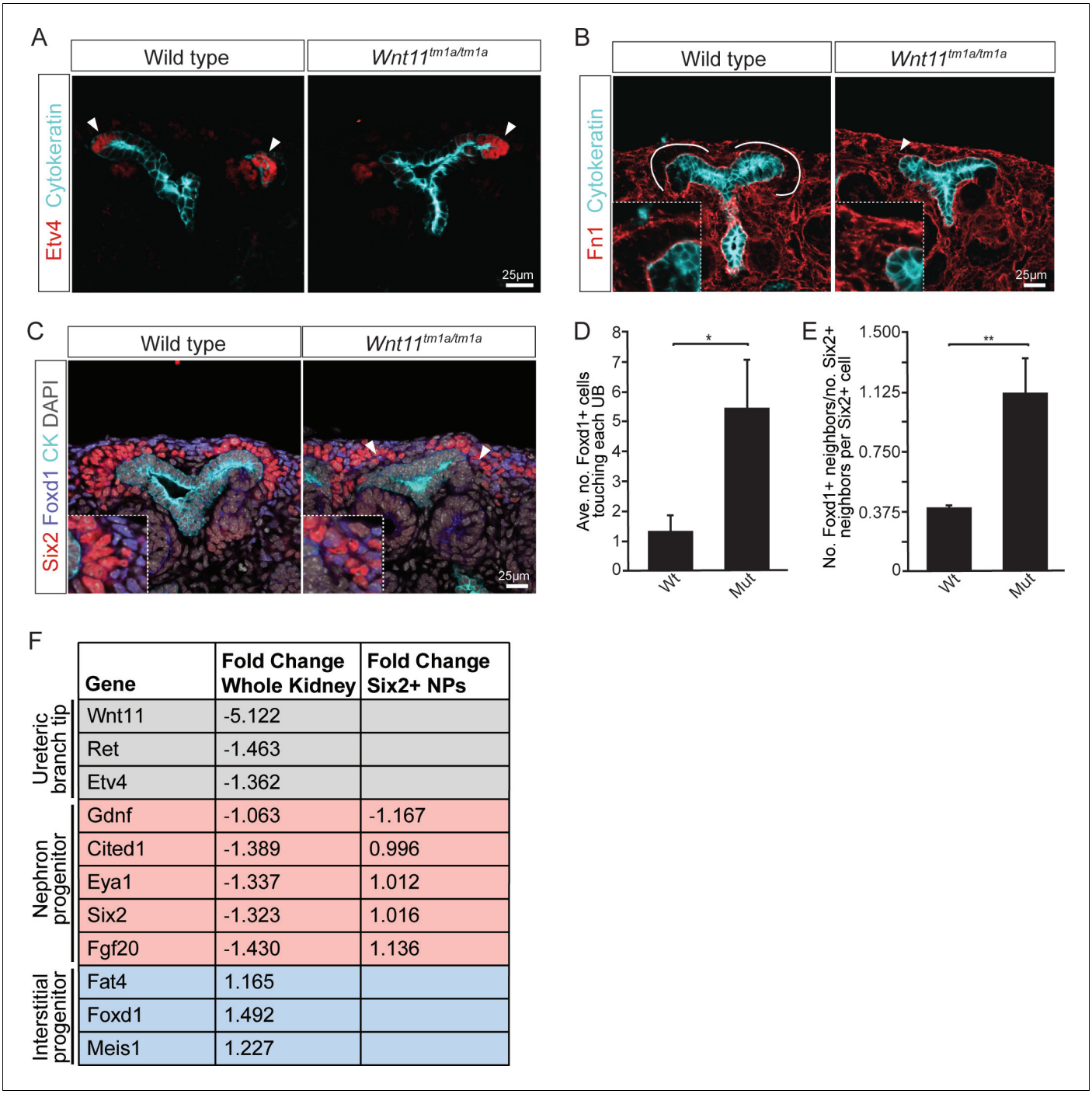

F

	Gene	Fold Change Whole Kidney	Fold Change Six2+ NPs
Ureteric branch tip	Wnt11	-5.122	
	Ret	-1.463	
	Etv4	-1.362	
Nephron progenitor	Gdnf	-1.063	-1.167
	Cited1	-1.389	0.996
	Eya1	-1.337	1.012
	Six2	-1.323	1.016
	Fgf20	-1.430	1.136
Interstitial progenitor	Fat4	1.165	
	Foxd1	1.492	
	Meis1	1.227	

Figure 4. Nephron progenitors intermix with interstitial progenitors but no significant changes in gene expression are observed. (**A**) E15.5 kidneys were sectioned and immunostained for the tip marker Etv4 (red) and cytokeratin (cyan). Distinct ureteric branch tip domains are still present in *Wnt11* mutants as indicated (arrowheads). (**B**) E15.5 sections were stained for the matrix protein fibronectin (Fn1; red) and cytokeratin (cyan). Note the exclusion of fibronectin from the nephron progenitor niche in wild type animals (line marks boundary between the nephron progenitors and interstitial progenitors). In *Wnt11*$^{tm1a/tm1a}$ kidneys the fibronectin boundary is disrupted and staining observed in the nephron progenitor niche (arrowheads). Insets show zoomed view of the progenitor niche. (**C**) Immunolocalization of Foxd1 +interstitial progenitors (blue) in conjunction with Six2 +nephron progenitors (red) at E15.5 reveals mixing of the two cell populations in *Wnt11* mutant kidneys (insets show zoomed view of cell mixing). Foxd1 +cells can infiltrate (arrowheads) the nephron progenitor niche and are found near the ureteric branch tips (cyan). (**D**) Quantitation of tissue sections immunostained for both Six2, Foxd1, and cytokeratin. There is an increase in the number of Foxd1 +cells touching the ureteric branch tips in Wnt11 mutants. 30 ureteric tip domains from n = 3 biological replicates were quantified. (**E**) Quantitation of Six2 cell neighbors. The number of Foxd1 +cells touching a Six2 +cell is divided by the number of Six2 +cells touching the same cell. In *Wnt11* mutants a Six2 +cell is just as likely to have as many

Figure 4 continued on next page

Figure 4 continued

Foxd1 +neighbors as Six2 +neighbors. Three biological replicates were quantified, 10 Six2 +cells per sample. (**F**) Fold-changes associated with RNA-seq of either whole kidneys or Six2 +cells from wild type and *Wnt11* mutant kidneys. The fold-change was calculated from the average of n = 6 for each genotype in whole kidney analysis and n = 3 for each genotype in the nephron progenitor analysis. Example genes which define each progenitor population (ureteric branch tip, nephron progenitor, and interstitial progenitor) are shown. No significant changes (>1.5 fold change) are observed. All error bars represent SEM. All significance values were determined by t-test. ns = $p > 0.05$, * = $p < 0.05$, ** = $p < 0.01$, *** = $p < 0.001$.

DOI: https://doi.org/10.7554/eLife.40392.012

A

Gene	RPKM in Six2+ cells
Ptk7	106
Fzd2	80
Ryk	45.69
Fzd7	25.22
Lrp6	24.69
Lrp10	20.44
Lrp5	19.22
Lrpap1	17.24
Fzd4	15.8
Vangl2	13.83
Lrp3	12.68
Fzd1	11.7
Celsr2	9.887
Lrp1	9.881
Lrp12	9.467
Fzd3	8.24
Celsr1	7.968
Lrp4	4.171
Lrp8	3.776
Ror2	3.349
Fzd8	3.139
Vangl1	2.459
Lrp2	2.168
Ror1	1.355
Fzd5	1.31

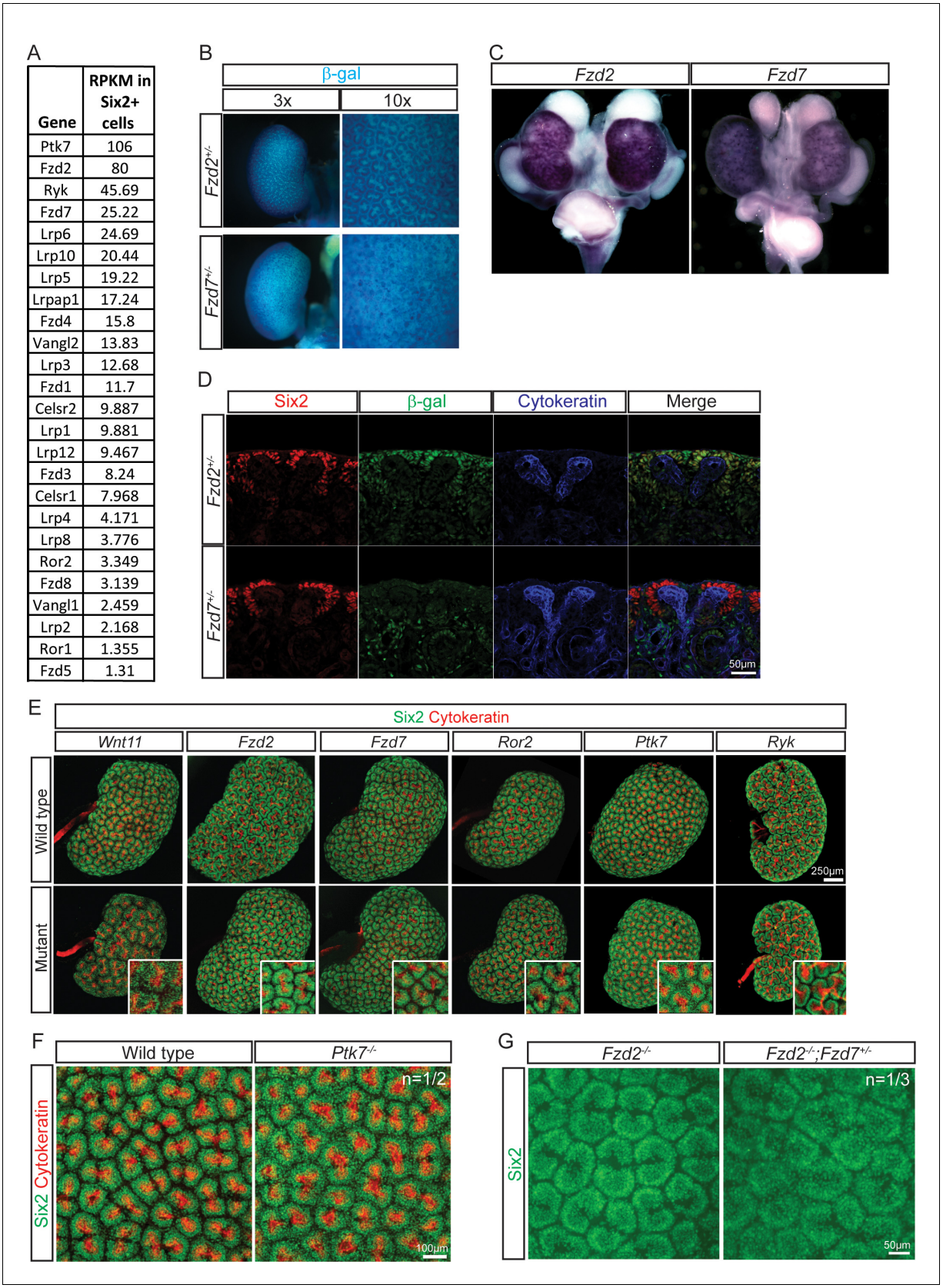

Figure 4—figure supplement 1. Several Wnt receptors are expressed in the nephron progenitors and display weakly penetrant phenotypes upon deletion. (**A**) RNA-seq from E16.5 Six2 +nephron progenitors reveals the expression of several Wnt pathway receptors and co-receptors. RPKM values

Figure 4—figure supplement 1 continued on next page

Figure 4—figure supplement 1 continued

are listed for each gene. Only genes with an RPKM >1 are shown. (**B**) β-galactosidase stains of *Fzd2*$^{+/-}$ and *Fzd7*$^{+/-}$ kidneys at E15.5. Alleles have a lacZ reporter inserted into the coding region. (**C**) Wholemount in situ hybridization for *Fzd2* and *Fzd7* on E15.5 urogenital systems show that they largely recapitulate the β-gal expression patterns. (**D**) Immunostaining for Six2 (red), β-galactosidase (green), and cytokeratin (blue) on E15.5 kidney sections from *Fzd2* and *Fzd7* heterozygous animals to show the expression domains of each receptor. Both are found within the nephron progenitors, but *Fzd7* to a lesser extent. (**E**) Wholemount immunostains for Six2 (green) and cytokeratin (red) were performed on mutants and appropriate controls at E15.5 for each receptor listed (*Wnt11* is included for comparison). For *Ror2*, the conditional line was crossed to the *Six2TGC*^{tg} line to specifically remove *Ror2* in the nephron progenitors (*Ror2*$^{c/c}$;*Six2TGC*$^{tg/+}$). No receptor mutant completely recapitulates the *Wnt11* mutant phenotype. Insets show 2X magnification. (**F**) High resolution view shows the slightly disorganized Six2 +nephron progenitors (green) in E15.5 *Ptk7*$^{-/-}$ kidneys although cap boundaries are still visible and the phenotype only occurred in one of two mutants analyzed. (**G**) Wholemount immunostains for Six2 (green) on E15.5 kidneys from *Fzd2*$^{-/-}$ and *Fzd2*$^{-/-}$;*Fzd7*$^{+/-}$ ±. Slightly disorganized caps were observed in one of three kidneys examined.

DOI: https://doi.org/10.7554/eLife.40392.013

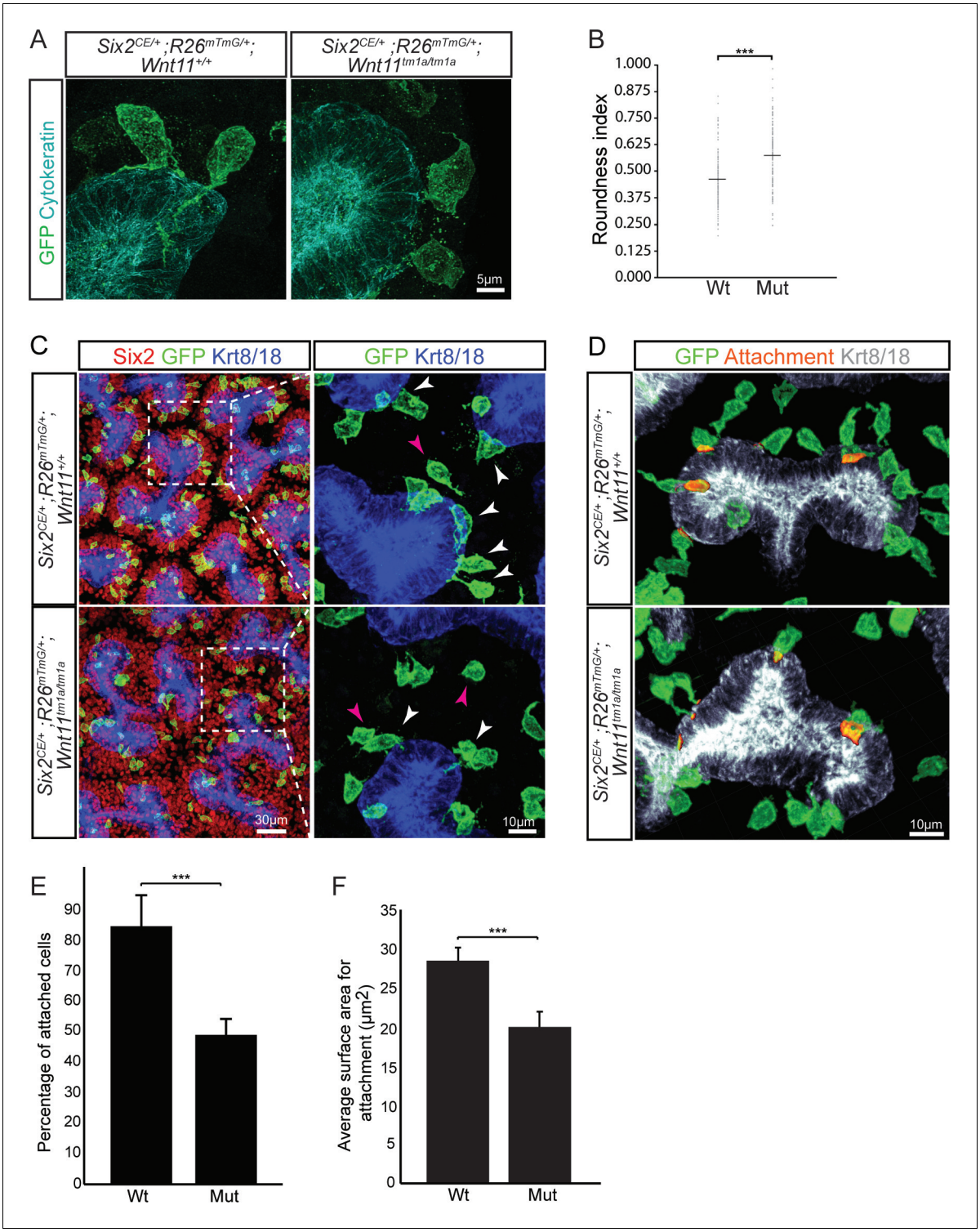

Figure 5. *Wnt11* mutants show a significant reduction in membranous attachments of nephron progenitors to the ureteric branch tip. (**A**) Sections from E15.5 *Six2*$^{CE/+}$; *R26*$^{mTmG/+}$; *Wnt11*$^{+/+}$ and *Six2*$^{CE/+}$; *R26*$^{mTmG/+}$; *Wnt11*$^{tm1a/tm1a}$ kidneys (recombination induced 24 hr prior) were immunostained for GFP (green) and cytokeratin (cyan) to visualize the GFP +cells in relation to the ureteric branch tips. Nephron progenitors make long, membranous projections which attach to the ureteric bud. Less extensive projections make contact with the ureteric branch tip in *Wnt11* mutants and appear rounder. (**B**) Quantitation of GFP +cell roundness from samples in A) (length/width = roundness index) reveals that *Wnt11* mutant nephron progenitors are rounder. n = 100 cells for each genotype. (**C**) Wholemount immunostains were carried out on E15.5 *Six2*$^{CE/+}$; *R26*$^{mTmG/+}$; *Wnt11*$^{+/+}$ and *Six2*$^{CE/+}$; *R26*$^{mTmG/+}$; *Wnt11*$^{tm1a/tm1a}$ kidneys (recombination induced 24 hr prior) for Six2 (red), GFP (green), and cytokeratin 8/18 (Krt8/18; blue). Confocal images

Figure 5 continued on next page

Figure 5 continued

show the dispersion of GFP +cells within the Six2 +nephron progenitor niche. Magnified views point to attached (white arrowhead) and detached (pink arrowhead) cells, with more detached cells present in *Wnt11* mutants. (**D**) Kidneys similar to those from C) showing the overlay of GFP (green) and Krt8/18 (grey) signal as an area of attachment (orange). More extensive areas of attachment are observed in wild type kidneys. (**E**) Quantitation of attachments from samples similar to C) showing a significant reduction in the percentage of attached cells in Wnt11 mutants. n = 200–400 cells from each of 4 biological replicates were analyzed. (**F**) Quantitation of attachment area as shown in D). The average surface area of attachments is reduced in *Wnt11* mutants. All error bars represent SEM. All significance values were determined by t-test. ns = $p > 0.05$, * = $p < 0.05$, ** = $p < 0.01$, *** = $p < 0.001$.

DOI: https://doi.org/10.7554/eLife.40392.015

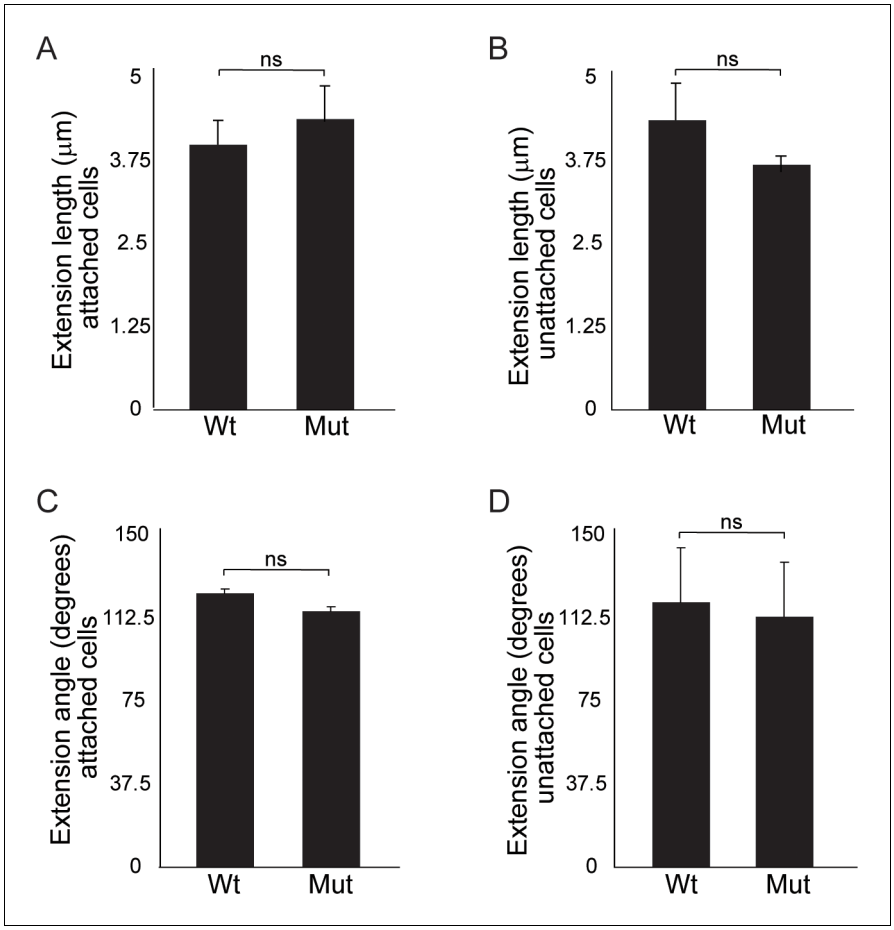

Figure 5—figure supplement 1. Quantitation of cellular extensions reveals no significant differences between wild type and *Wnt11* mutant nephron progenitors. (**A**) Average extension lengths for attached nephron progenitor cells. (**B**) Average extension length for unattached nephron progenitors. (**C**) Angle of the extension relative to the ureteric bud for attached nephron progenitors. (**D**) Angle of extension relative to the ureteric bud for unattached nephron progenitors. An average of 20 cells from three replicates were analyzed. All error bars represent SEM. All significance values were determined by t-test. ns = $p > 0.05$, * = $p < 0.05$, ** = $p < 0.01$, *** = $p < 0.001$.
DOI: https://doi.org/10.7554/eLife.40392.016

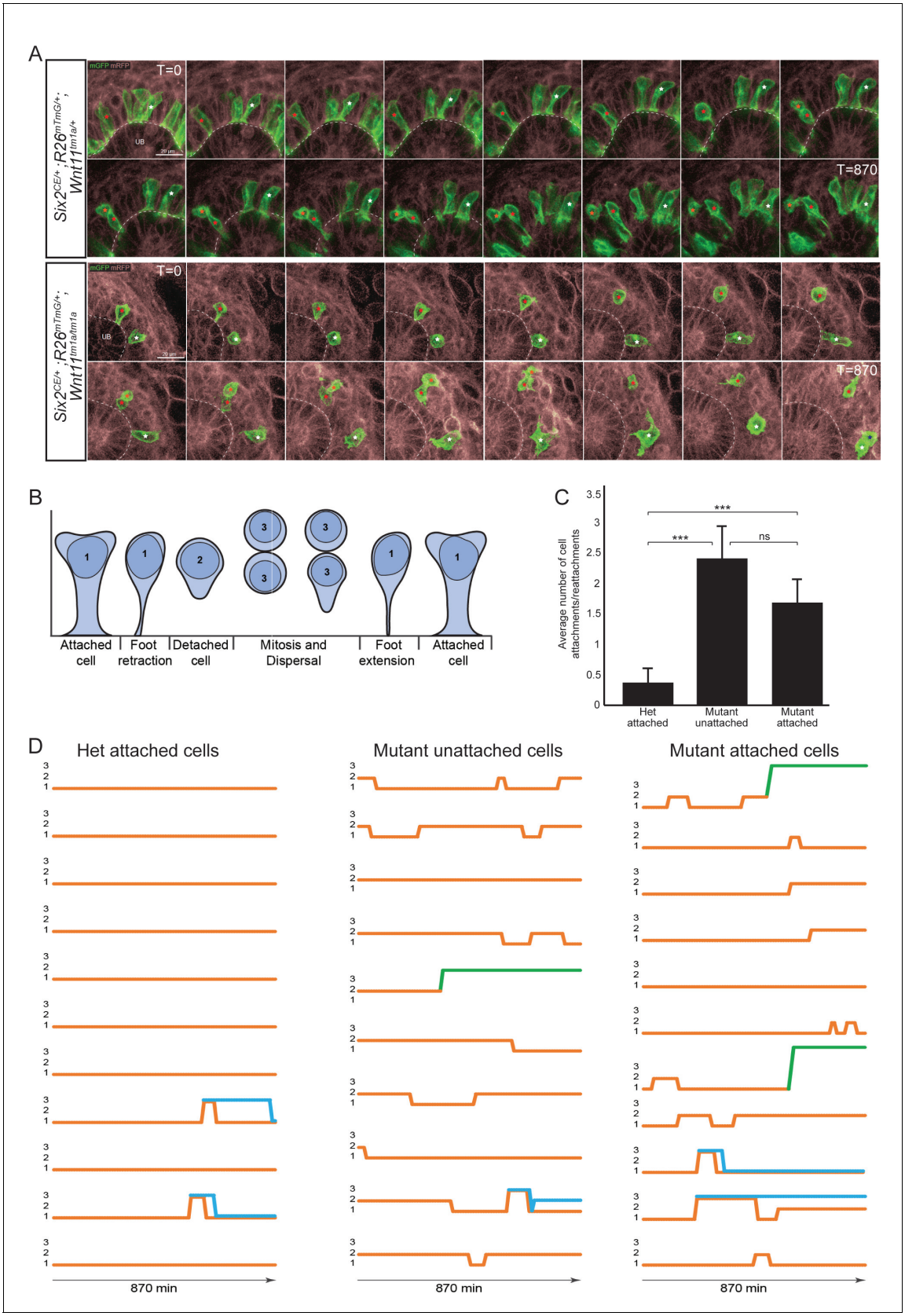

Figure 6. The nephron progenitors of *Wnt11* mutants display dynamic attachments and reattachments to the ureteric bud. (**A**) Still images from *Six2*$^{CE/+}$; *R26*$^{mTmG/+}$; *Wnt11*$^{tm1a/+}$ and *Six2*$^{CE/+}$; *R26*$^{mTmG/+}$; *Wnt11*$^{tm1a/tm1a}$ kidney explant cultures live-imaged over 870 min (14.5 hr). GFP +cells are in

Figure 6 continued on next page

Figure 6 continued

green, the tdTomato +membrane of all other cells is in grey. Two cells are marked with an asterisk (red or white) in each genotype and followed across the time. The cells marked with red asterisk go through a cell division, the white cells do not. In the control kidneys, the white cell stays attached throughout. The red cell detaches briefly to divide and quickly reattaches. In *Wnt11* mutants, both cells display dynamic attachments and reattachments. (**B**) Schematic of the classification scheme utilized to define cellular dynamics of the nephron progenitors. (**C**) Quantitation of the average number of attachments and reattachments of cells during live imaging. All het control cells generally begin attached and display few attachments/reattachments. *Wnt11* mutant cells, whether they were attached or detached when imaging began, both display numerous attachments/reattachments. (**D**) Representative tracks of 10–11 individual cells classified as in B) over the course of live imaging. 11 control and 33 mutant cells were analyzed in total. Orange tracks highlights the transition between stages. Control cells stayed attached and only detached to divide. Mutant cells, whether initially attached or detached, show dynamic movements. Blue track = new cell from a division. Green = cell migrated out of the imaging field. All error bars represent SEM. All significance values were determined by t-test. ns = $p > 0.05$, * = $p < 0.05$, ** = $p < 0.01$, *** = $p < 0.001$.

DOI: https://doi.org/10.7554/eLife.40392.019

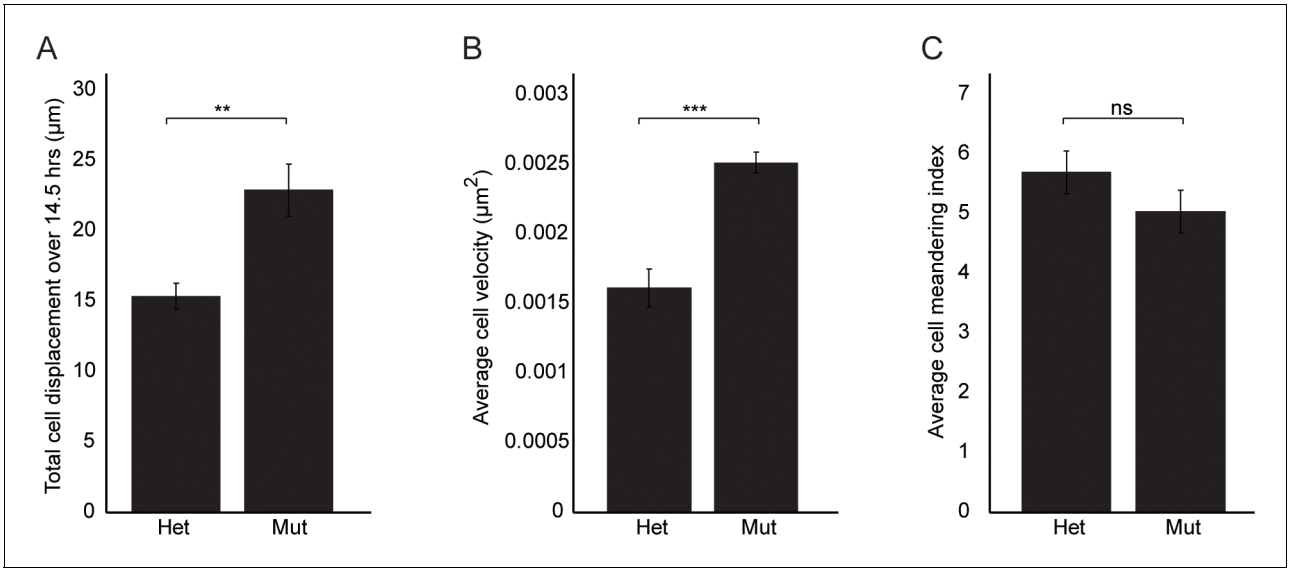

Figure 6—figure supplement 1. *Wnt11* mutant nephron progenitors show greater displacement and velocities, but meander similarly to wild type cells. (**A**) Total cell displacement was measured for *Six2*$^{CE/+}$; *R26*$^{mTmG/+}$; *Wnt11*$^{tm1a/+}$ and *Six2*$^{CE/+}$; *R26*$^{mTmG/+}$; *Wnt11*$^{tm1a/tm1a}$ nephron progenitors imaged for 870 min (14.5 hr). GFP +cells were tracked and the total distance they moved recorded. *Wnt11* mutant cells show greater displacement. (**B**) The average velocity of nephron progenitors was quantitated and *Wnt11* mutant nephron progenitors display greater average speeds when moving. (**C**) The cell meandering index was calculated and *Wnt11* mutants meander similarly to wild type cells. 87 control cells and 62 mutant cells were analyzed for all quantifications. All error bars represent SEM. All significance values were determined by t-test. ns = $p > 0.05$, * = $p < 0.05$, ** = $p < 0.01$, *** = $p < 0.001$.

DOI: https://doi.org/10.7554/eLife.40392.020

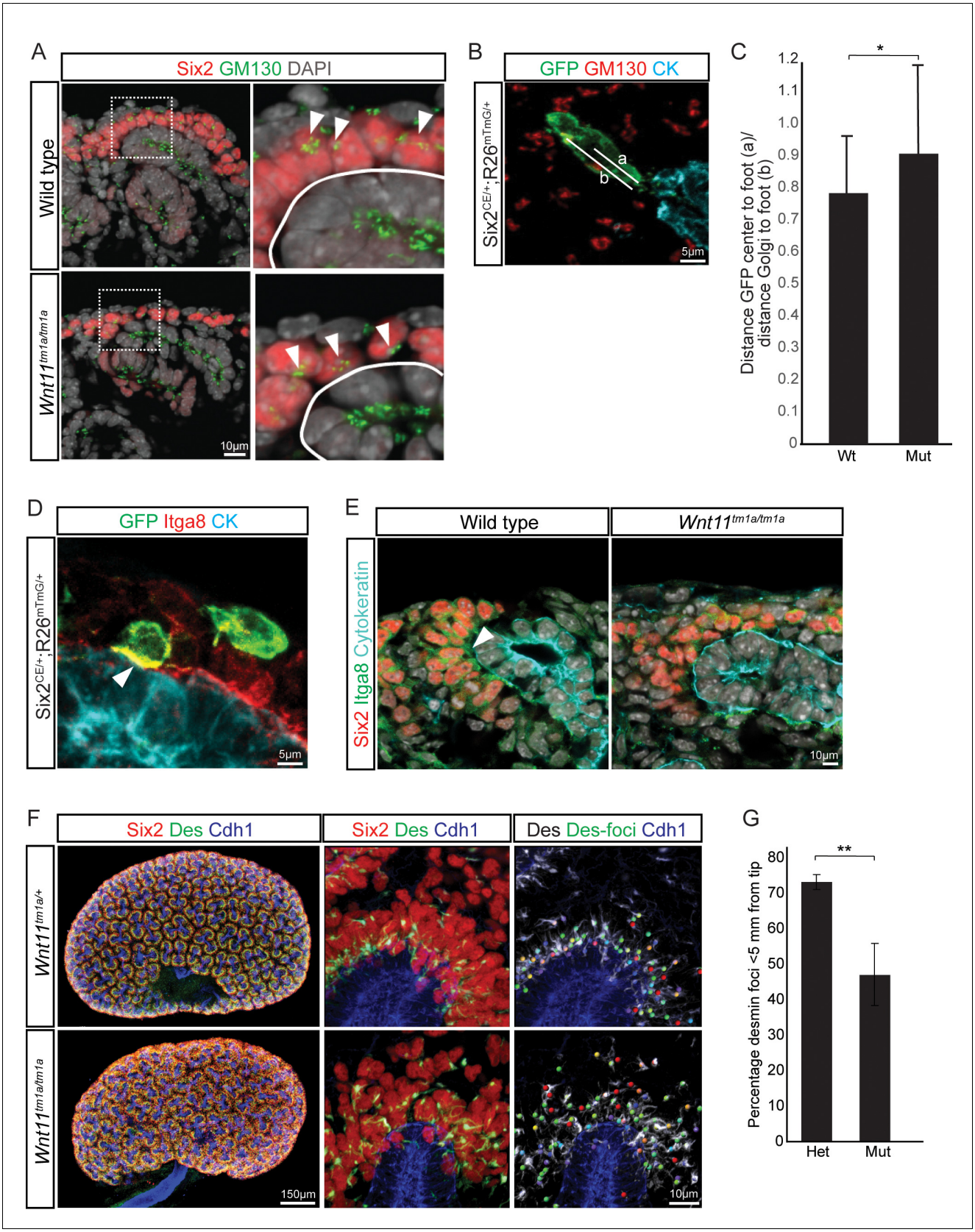

Figure 7. Nephron progenitor polarity is disrupted in *Wnt11* mutants. (**A**) E15.5 kidney sections were immunostained for Six2 (red), GM130 (Golgi; green) and DAPI (grey). The Golgi (white arrowheads) show a polarization to the distal end of nephron progenitors in wild type kidneys and this

Figure 7 continued on next page

Figure 7 continued

polarization is disrupted in *Wnt11* mutants where they are localized closer to the ureteric branch tip (white outline). (**B**) Staining for GFP (green), GM130 (red), and cytokeratin (cyan) highlighting the normal polarization of Golgi within the nephron progenitor at E15.5. The letter 'a' marks the distance from the cell center to the foot of the cell (contact with tip) and 'b' marks the distance from the Golgi to the foot. (**C**) Ratio of the distances described in B) for wild type and mutant cells. Wild type cells show a smaller ratio indicating the Golgi lie farther from the ureteric tip than *Wnt11* mutant cells, supporting their polarized nature and the loss in *Wnt11* mutants. Three biological replicates and ~20 cells from each replicate were quantified. (**D**) E15.5 kidney sections immunostained for GFP (green), integrin a8 (Itga8; red) and cytokeratin (CK, cyan). Image shows the overlap of GFP +signal with Itga8 in cells close to the tip (white arrowhead), suggesting polarization of Itga8. (**E**) E15.5 kidney sections immunostained for Six2 (red), Itga8 (green), and cytokeratin (cyan). Arrowhead points to Itga8 polarization towards the ureteric branch tip in wild type kidneys, which is lost in *Wnt11* mutants. (**F**) E15.5 wholemount immunostains for Six2 (red), desmin (Des; green), and cadherin 1 (Cdh1; blue) show the polarization of desmin foci (Des-foci) toward the ureteric branch tip which is disrupted in *Wnt11* mutant kidneys. Since the desmin stain appears aster-like with wispy projections, the central focal point (foci) were identified for ease of distance quantitation. Foci were automatically located by Imaris imaging software as the most intense focal point of the desmin stain. (**G**) Quantitation of the percentage of desmin foci located greater than 5 μm from the ureteric tip in each genotype showing the greater dispersion from the tip in *Wnt11* mutants. 385 foci from five control tips and 353 foci from four tips were analyzed. All error bars represent SEM. All significance values were determined by t-test. ns = $p > 0.05$, * = $p < 0.05$, ** = $p < 0.01$, *** = $p < 0.001$.

DOI: https://doi.org/10.7554/eLife.40392.024

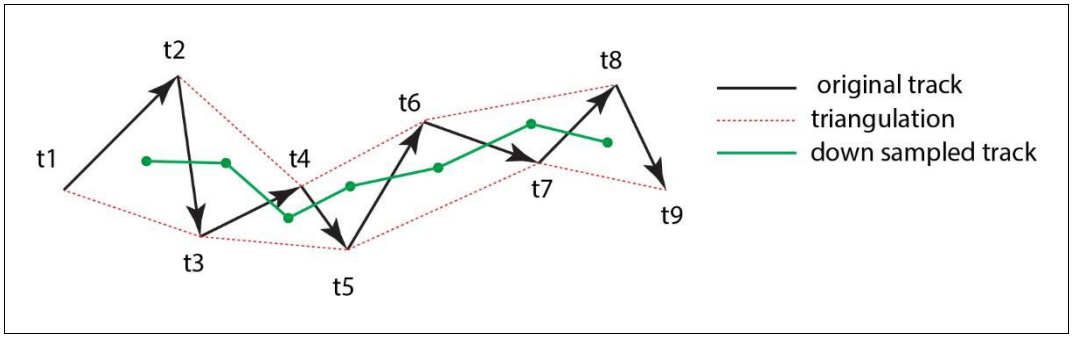

Figure 8. Triangulation to improve accuarcy of cell tracking. Schematic showing the method of triangulaton used to improve the accuracy of tracking nephron progenitors.

DOI: https://doi.org/10.7554/eLife.40392.025